



**RESEARCH LETTER**

10.1029/2018GL080225

**Key Points:**

- We analyzed the propagation of climatic signals to Holocene sediment records of three well-studied Tibetan lakes in a dynamical system framework
- Holocene variation in geochemical proxies mainly reflect site-specific landscape responses to abrupt climate change
- Our results indicate a feedback between physical and chemical erosion processes on interglacial timescale

**Supporting Information:**

- Supporting Information S1

**Correspondence to:**

A. Ramisch,  
arne.ramisch@gfz-potsdam.de

**Citation:**

Ramisch, A., Tjallingii, R., Hartmann, K., Diekmann, B., & Brauer, A. (2018). Echo of the Younger Dryas in Holocene lake sediments on the Tibetan Plateau. *Geophysical Research Letters*, 45. <https://doi.org/10.1029/2018GL080225>

Received 26 AUG 2018

Accepted 7 OCT 2018

Accepted article online 11 OCT 2018

**Echo of the Younger Dryas in Holocene Lake Sediments on the Tibetan Plateau**

**Arne Ramisch<sup>1</sup> , Rik Tjallingii<sup>1</sup> , Kai Hartmann<sup>2</sup> , Bernhard Diekmann<sup>3,4</sup>, and Achim Brauer<sup>1,4</sup>**

<sup>1</sup>Section 5.2: Climate Dynamics and Landscape Evolution, GFZ German Research Centre for Geosciences, Potsdam, Germany, <sup>2</sup>Department of Earth Sciences, Institute of Geographical Science, Freie Universität Berlin, Germany, <sup>3</sup>Alfred-Wegener-Institute Helmholtz Centre for Polar and Marine Research, Potsdam, Germany, <sup>4</sup>University of Potsdam, Institute of Earth and Environmental Science, Germany

**Abstract** Reading the sediment record in terms of past climates is challenging since linking climate change to the associated responses of sedimentary systems is not always straightforward. Here we analyze the erosional response of landscapes on the Tibetan Plateau to interglacial climate forcing. Using the theory of dynamical systems on Holocene time series of geochemical proxies, we derive a sedimentary response model that accurately simulates observed proxy variation in three lake records. The model suggests that millennial variations in sediment composition reflect a self-organization of landscapes in response to abrupt climate change between 11.6 and 11.9 ka BP. The self-organization is characterized by oscillations in sediment supply emerging from a feedback between physical and chemical erosion processes, with estimated response times between 3,000 to 18,000 years depending on catchment topography. The implications of our findings emphasize the need for landscape response models to decipher the paleoclimatic code in continental sediment records.

**Plain Language Summary** Lake sediments are an important source of information on past climates. Reading the information is not always straightforward. Complex interactions in landscapes can affect the transmission of climatic signals to the sediment record. However, the exact nature of such complex interactions remains unknown. This study compares sediment deposits of three lakes on the Tibetan Plateau. The deposits are continuous records of landscape responses to climate change during the last 12,000 years. We identified a mathematical model that accurately simulates changes in sediment composition at all sites. The model simulations suggest that an abrupt warming at the end of the last glacial period destabilized the landscapes. This caused fluctuations in the transport of sediments, which persisted for several thousand years. Our findings present evidence for a long-lasting impact of abrupt climate change on fundamental Earth surface processes.

**1. Introduction**

Understanding sedimentary responses of landscapes to climate forcing is the key to decode paleoclimatic information from sediment proxy records. Regional comparisons of proxy records often show differentiated long-term sedimentation patterns (Engstrom et al., 2000; Ott et al., 2017; Roberts et al., 2016; Wischniewski et al., 2011), suggesting variable sedimentary responses of landscapes to climate forcing. This divergence of climate signals is commonly explained by site-specific fluctuations in sediment supply (Allen, 2008a; Jerolmack & Paola, 2010; Romans et al., 2016). These fluctuations emerge from interactions between sedimentary processes in landscapes, such as feedbacks between the dissolution and erosion of regolith covers (Ferrier & Kirchner, 2008; Gabet & Mudd, 2009; Heimsath, 2012) or the incision and aggradation of alluvial surfaces (Dalman et al., 2015; Kim & Jerolmack, 2008). Consequently, climatic perturbations can destabilize landscape configurations and induce variations in sediment supply, which reflect self-organizations of coupled sedimentary process systems rather than variations in external forcing. So far, attempts to identify interactions in coupled sedimentary process systems and their response times to external forcing focused on experimental and simulated landscapes (e.g., Armitage et al., 2011, 2013; Bonnet & Crave, 2003; Humphrey & Heller, 1995). However, the heterogeneity of natural landscapes (Phillips, 2007) impedes the application of general erosion and transport laws for climate reconstructions.

A crucial step toward applicable sedimentary response models for climate reconstructions is the identification of models from sediment record observations. Holocene lake sediments offer ideal archives that

©2018. The Authors.

This is an open access article under the terms of the Creative Commons Attribution-NonCommercial-NoDerivs License, which permits use and distribution in any medium, provided the original work is properly cited, the use is non-commercial and no modifications or adaptations are made.

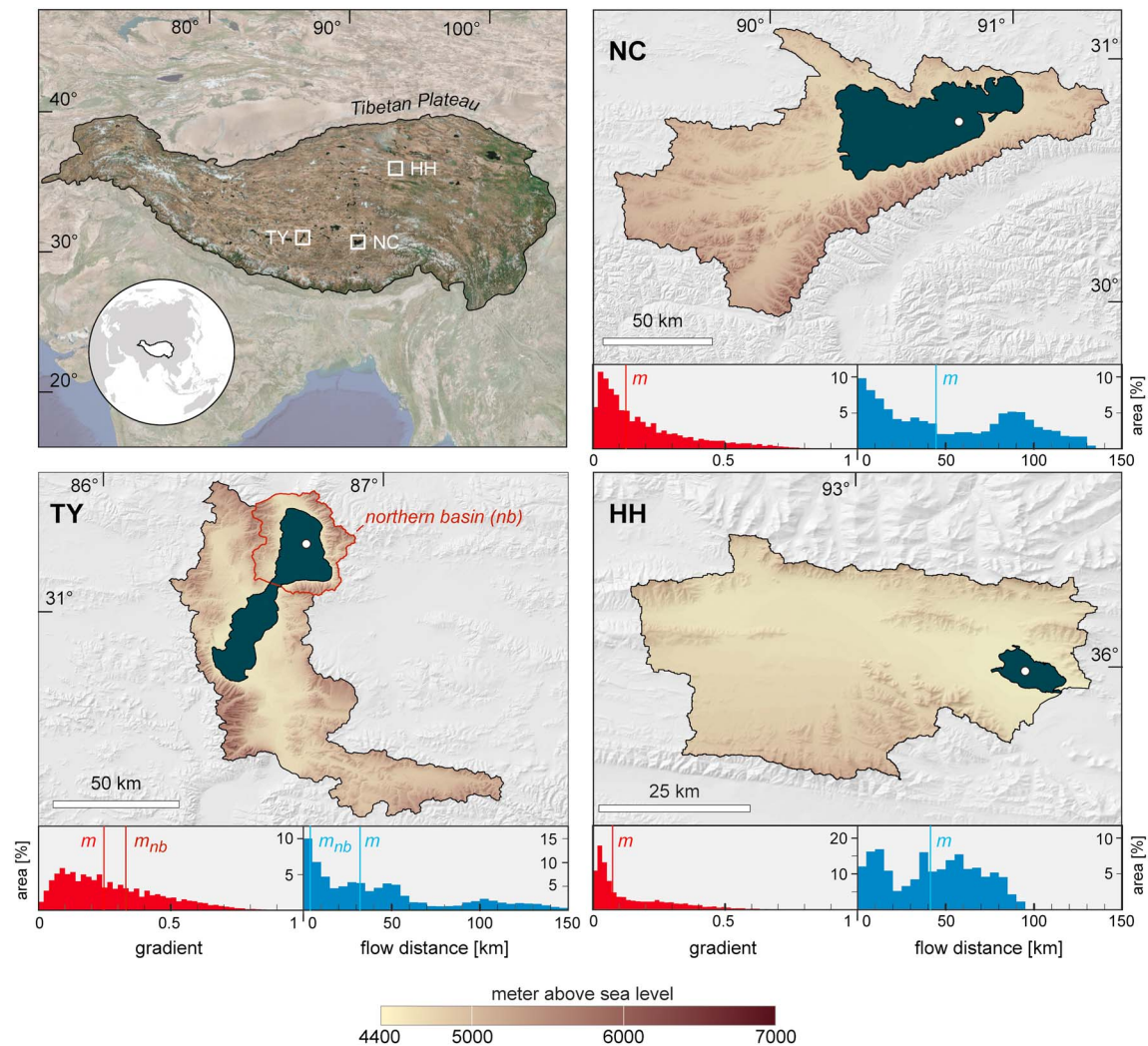


**Figure 1.** Study sites on the Tibetan Plateau including locations and drainage basins of the lakes Nam Co (NC), Tangra Yumco (TY), and Heihai (HH). Digital elevation models are based on Shuttle Radar Topography Mission data in 90-m resolution (Jarvis et al., 2008). Frequency distributions of slope gradients (red bars) and flow distances (blue bars) are normalized to catchment areas ( $m$  = median). Surface topography differs considerably among the three drainage basins, which influences sediment transport to the core locations (white dot). Due to the strong topographic differentiation of the catchment area of TY, normalization is also indicated for northern subbasin only ( $m_{nb}$ ).

record the interplay between sedimentary processes in their drainage basins, due to the good chronological control and wide geographical distribution. Here we analyze the sedimentary responses of erosional landscapes to interglacial climate forcing by comparing Holocene sediment records of three well-studied lake systems on the Tibetan Plateau. Using the theory of dynamical systems (e.g., Strogatz, 2001) on geochemical proxy time series, we derived a response model for sediment supply processes that accurately simulates Holocene variations in each record. The model is used to quantify interactions and response times of sediment supply processes at each site and to elucidate the propagation of climatic signals to the lacustrine records. We show that the diverging Holocene proxy records reflect site-specific responses in sediment supply to abrupt climate change at the end of the Younger Dryas cold period.

## 2. Data and Methods

We compared Holocene proxy records of three Tibetan lakes (Figure 1) that are situated in similar environmental conditions (supporting information S9): Lake Nam Co (NC), Lake Tangra Yumco (TY), and Lake Heihai (HH). All lake locations are influenced by the Asian Summer Monsoon circulation with main precipitation occurring during boreal summer. The semiarid climate conditions and high altitude cause a sparse

vegetation cover characterized by alpine steppe around all lakes (Lu et al., 2010; Mieke et al., 2014; Müller & Kürschner, 2014). All catchments are dominated by granitoid to metamorphic bedrock lithology (Akita et al., 2015; Kasper et al., 2012; Stauch et al., 2017), with subordinate occurrences of carbonate outcrops at Lake NC (Kasper et al., 2012) and HH (Ramisch et al., 2016). The main differentiation between the lakes is the topographic setting of the surrounding landscapes, which differ in slope gradients (TY > NC > HH) and the average distance for fluvial transport processes (NC > HH > TY) in the drainage basins (Figures 1b–1d). This results in a high topographic efficiency for erosion and transport processes at TY, a moderate efficiency at NC, and a low efficiency at HH.

### 2.1. Generating Time Series of Sedimentary Processes

Nondestructive X-ray fluorescence (XRF) core scanning records are measured directly at the split core sediment surface and provide geochemical element intensity records (in counts per second). The XRF scanning record of HH was measured every 0.5 cm with 10 and 30 kV using an Avaatech XRF core scanner at the Alfred Wegener Institute for Polar and Marine Research in Bremerhaven (Germany). The sediment core records of HH, NC (Doberschütz et al., 2014; Kasper et al., 2012), and TY (Ahlborn et al., 2017) provide intensity records of the eight elements Al, Si, K, Ca, Ti, Fe, Sr, and Rb.

Analyzing the variation in sediment compositions by using element intensity records (in counts per second) obtained by XRF core scanning can be problematic due to the poorly constrained measurement geometry (e.g., variable water content, grain-size distribution, or density) and nonlinear matrix effects (e.g., Tjallingii et al., 2007). However, log-ratios of element intensities are linear functions of log-ratios of concentrations and provide the most easily interpretable signals of relative changes in chemical composition (Weltje & Tjallingii, 2008). Additionally, log-ratios of element intensities are consistent with the statistical theory of compositional data analysis (Aitchison, 1982, 1986), which allows robust statistical analyses in terms of sediment compositions (Weltje et al., 2015). Therefore, prior to statistical analyses, element intensities (intensity  $I$  of sample  $i$  and element  $j$  for  $D$  elements) were center-log-ratio transformed by

$$clr_j(i) = \ln \left( \frac{I_{ij}}{\sqrt[D]{\prod_{j=1}^D I_{ij}}} \right) \quad (1)$$

We use a principle component analysis to explore the relative correlations and interdependencies between individual elements (Figure S1 in the supporting information). The elements dominating the variance of the XRF records (PC1) have been selected for calculation of additive log-ratios ( $alr$ ; intensity  $I$  of measurement  $i$  for elements  $j$  and  $k$ ) by

$$alr(i) = \ln \left( \frac{I_{ij}}{I_{ik}} \right) \quad (2)$$

The chronology for the  $alr$  time series of each lake was established using accelerator mass spectrometry  $^{14}\text{C}$  dating on 24 bulk sediment samples for Lake NC (Doberschütz et al., 2014), 27 bulk sediment samples for Lake TY (Haberzettl et al., 2015; Henkel et al., 2016), and 19 samples of macro plant remains for Lake HH (Lockot et al., 2015). The sediment record of Lake TY is interrupted by several event-related layers that impede a continuous age-depth association due to a disproportionate sediment accumulation in relatively short time intervals. Therefore, we used the event corrected composite depth scale of Lake TY as presented by Henkel et al. (2016).  $^{14}\text{C}$  dating approaches on the Tibetan Plateau are often hindered by pronounced reservoir carbon within the water column (Mischke et al., 2013), causing an overestimation of radiocarbon ages due to the reservoir effect. Comparisons of paleomagnetic secular variations inferred from sediments of lake NC and TY with geomagnetic field models (Haberzettl et al., 2015) as well as optically stimulated luminescence dating of core samples (Long et al., 2015) suggest a nearly constant reservoir effect during the Holocene for Lake TY and Lake NC. Accelerator mass spectrometry  $^{14}\text{C}$  dates and paleomagnetic secular variations within the record of Lake HH, in turn, indicate a gradual increase of the reservoir effect since ~8.0 ka BP, leading to four probable age-depth relationships (models 1–4) inferred from a process and provenance modeling approach (Lockot et al., 2015). This study uses age-depth relations provided by models 3 and 4 with an average reservoir effect between 3 and 4 ka, which is supported by comparisons between optically stimulated luminescence and  $^{14}\text{C}$  dating of mid-Holocene high-stand sediments (An et al., 2018). Despite the reasonable

correspondence between independent dating techniques in all records, we restrict our analysis to millennial variations.

## 2.2. Sedimentary Response Model Identification

To identify a suitable sedimentary response model from geochemical time series, we adapted a dynamical system approach. Dynamical system theory offers the mathematical framework to analyze the temporal evolution of systems that exhibit interactions between their subcomponents (called system variables) such as landscapes. For a comprehensive introduction to the field of dynamical systems, see, for example, Strogatz (2001). Following the notation of Strogatz (2001), the temporal evolution ( $\dot{x} \equiv dx/dt$ ) of a system variable ( $x_i$ ) is a function of the states of all system variables ( $x_1, \dots, x_n$ ), represented in the general mathematical system of coupled differential equations by

$$\begin{aligned}\dot{x}_1 &= f_1(x_1, \dots, x_n) \\ &\vdots \\ \dot{x}_n &= f_n(x_1, \dots, x_n)\end{aligned}\tag{3}$$

A convenient method to solve such a system geometrically (instead of analytically) is to visualize the temporal evolution of the system in a so-called phase space. The phase space is an abstract space, in which each axis represents all possible states of a system variable. Consequently, a point in phase space characterizes the states of all system variables at time  $t$ . The temporal evolution of the system will follow a trajectory in phase space, in which the geometry of the trajectory is completely determined by the interactions between the system variables.

Scalar sequences of measurements such as *alr* time series offer only a one-dimensional view on the underlying dynamics of a system. Packard et al. (1980) and Takens (1981) introduced and formalized a methodological approach to reconstruct higher dimensional phase spaces from one-dimensional time series. This standard approach for phase space reconstruction from a time series involves associating a scalar measurement at time  $t$  with past values to form a new state vector  $\vec{v}(t)$ . Specifically, we used this embedding-delay method to reconstruct the  $n$ -dimensional state vector  $\vec{v}(t)$  for *alr*( $t$ ) by  $n$  time delayed *alr* measurements:

$$\vec{v}(t) = [alr(t), alr(t + \tau), \dots, alr(t + (n - 1)\tau)]\tag{4}$$

with a fixed time delay  $\tau$ . Although not identical, the reconstruction is guaranteed to preserve the topology of the full dynamics and enables conclusions on the general dynamical properties of the system (Bradley & Kantz, 2015). Since applying equation (4) requires an evenly spaced *alr* time series, we resampled the original time series to 10-year resolution using a nearest neighbor interpolation. To estimate a suitable time delay  $\tau$  that maximizes linear independence between the coordinates of  $\vec{v}(t)$ , we used the first root of the autocorrelation function of *alr*( $t$ ). The number of system variables  $n$  was estimated using the false nearest neighbor classification (Kennel et al., 1992) and provided by the cross recurrence plot toolbox (Marwan et al., 2007) for Matlab.

## 3. Results

The dominant variance of the XRF records (PC1; see supporting information Figure S1) reveals a similar correlation for all three lakes between allogenic siliciclastic sediments (Al, Si, K, Ca, Ti, and Rb) and authigenic calcites (Ca and Sr). This variation in the XRF data has been linked to the supply of clastic particles by surface runoff for lakes NC (Doberschütz et al., 2014; Kasper et al., 2012) and TY (Ahlborn et al., 2017), whereas authigenic calcites precipitate within the lake. The variance within the siliciclastic elements (PC2) is probably related to the mineralogy and grain size of the detrital sediments in each lake. However, the main geochemical variations in all records are expressed by a negative correlation between the deposition of siliciclastic and authigenic sediments (PC1), which explain 73.1% (HH), 57.5% (TY), and 65.2% (HH) of total variance in the XRF records.

We analyzed variations in siliciclastic and authigenic sediment deposition in the temporal domain as represented by *alr* time series (*alr*( $t$ )) for each element combination indicative for variations in PC1 (see supporting information Figures S2–S4). The Holocene sequences exhibit similar temporal patterns, albeit differing in timing. Starting at low values in all time series during the Early Holocene, *alr* increase and begin to oscillate

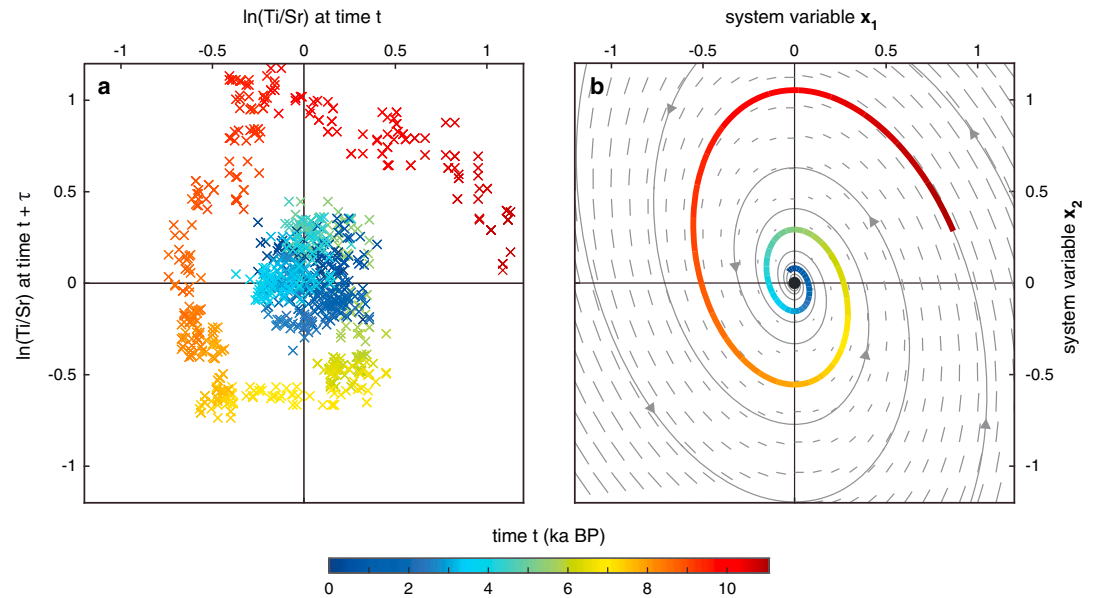


**Figure 2.** Reconstructed and modeled phase space trajectories for  $\ln(\text{Ti}/\text{Sr})$  time series of Lake Nam Co (NC). (a) Reconstructed phase space trajectory of  $\ln(\text{Ti}/\text{Sr})$  from the delay-coordinate embedding method with a constant time-lag of 1.05 ka. (b) Phase space portrait for the identified response model. A slope field (gray lines) indicates the direction of change resulting from the interactions between the system variables  $x_1$  and  $x_2$  (equation (5)) at each point in phase space. Coloring indicates the temporal evolution of the trajectory for the best-fit parameter combination of NC.

between high and low values. These oscillations dissipate over time, causing a settling of values to a stable state of low variability. The main difference between the three sites is the period of oscillations ( $\text{HH} > \text{NC} > \text{TY}$ ). Such site-specific oscillatory decay refutes a direct forcing of regional hydroclimate on sedimentation patterns but rather indicates dynamical responses in the millennial-scale sedimentary evolution.

The identification of a suitable response model for the site-specific sedimentation patterns was based on reconstructed phase space trajectories for temporal variations in PC1. We chose *alr* time series of Ti and Sr to represent temporal variations in PC1 in terms of geochemical variation due to consistent negative correlations between Ti and Sr in all three records (supporting information S1). The results of the false nearest neighbor classification of  $\ln(\text{Ti}/\text{Sr})$  time series indicate a minimum of two system variables needed to model Holocene variations in each record (supporting information S8). The reconstructed  $\ln(\text{Ti}/\text{Sr})$  trajectories show a similar geometry (supporting information S5), most clearly apparent in the trajectory of Lake NC presented in Figure 2. The Holocene trajectory follows an inward spiral toward a fixed point near the origin. Inward spirals in two-dimensional phase spaces indicate an interaction between two processes, in which dissipation directs the dynamics toward a steady state of low variability. The dynamics around the steady state are consistent with a linear dynamical system of two coupled differential equations, which in its general form is given by

$$\begin{aligned} \dot{x}_1 &= ax_1 + bx_2 \\ \dot{x}_2 &= cx_1 + dx_2 \end{aligned} \quad (5)$$

where  $a$ ,  $b$ ,  $c$ , and  $d$  are parameters quantifying the interaction between system variables  $x_1$  and  $x_2$ . The system will exhibit inward spirals toward a fixed point in phase space, if the parameter matrix

$$A = \begin{bmatrix} a & b \\ c & d \end{bmatrix} \quad (6)$$

is characterized by a positive determinant ( $\det(A) > 0$ ) and a negative trace ( $\text{tr}(A) < 0$ ) that satisfy  $\text{tr}(A)^2 - 4\det(A) < 0$  (Strogatz, 2001). The identified model accurately reproduces the Holocene dynamics in *alr* time series as indicated by the close correspondence between reconstructed (Figure 2a) and modeled (Figure 2b) trajectories of  $\ln(\text{Ti}/\text{Sr})$ .

To explore the role of external forcing in the response of the sedimentary systems, we formulated the general dynamical system (equation (5)) in a forcing-response structure. A standard forcing-response structure for linear dynamical systems is provided by linear time invariant (LTI) system models (e.g., Phillips et al., 1995). LTI system models simulate the response of a given linear system to an arbitrary forcing signal by expanding the system model (equations (5) and (6)) with a forcing ( $u(t)$ ) and output term ( $y(t)$ ). We used a second-order LTI system model to reproduce geochemical variability in the records with simulated  $alr$  time series ( $y(t) \equiv alr_{sim}(t)$ ) in response to a change in external forcing  $u(t)$ . The model is given in matrix notation by

$$\begin{pmatrix} \dot{x}_1 \\ \dot{x}_2 \end{pmatrix} = \begin{bmatrix} -2\zeta\omega_n & -\omega_n^2 \\ 1 & 0 \end{bmatrix} \begin{pmatrix} x_1 \\ x_2 \end{pmatrix} + \begin{bmatrix} k \\ 0 \end{bmatrix} u(t) \quad (7)$$

$$alr_{sim}(t) = \begin{bmatrix} 0 & \omega_n^2 \end{bmatrix} \begin{pmatrix} x_1 \\ x_2 \end{pmatrix}$$

where  $k$  denotes a factor to scale to the codomain of  $alr_{sim}$  to record observations. An abrupt change in external forcing is provided by unit step function ( $u(t)$ ) that is initiated at time  $t_i$  (in cal. ka BP). The LTI parameterization scheme encapsulates the response at each site in a natural oscillation frequency  $\omega_n$  (in radians per kilo year) and a relative damping factor  $\zeta$  (dimensionless). We iteratively estimated best fits for  $t_i$ ,  $\omega_n$ , and  $\zeta$  in  $10^6$  Monte Carlo simulations for each  $\ln(\text{Ti}/\text{Sr})$  time series in a least square approach. Because of the repeated occurrence of aragonite in the record of Lake HH,  $\ln(\text{Ti}/\text{Sr}) < -0.67$  were not considered in the modeling routine. Since the orthorhombic crystal lattice of aragonite favors Sr coprecipitation, a shift in the dominant authigenic mineral phase between calcite and aragonite results in sudden jumps in  $\ln(\text{Ti}/\text{Sr})$  time series, which are unrelated to the millennial scale dynamics of the records.

The results indicate an accurate match between proxy records and model simulations for millennial-scale dynamics during transient phases (Figures 3a–3f), with an average root mean square error of 0.18 (NC), 0.54 (TY), and 0.26 (HH). The initiations  $t_i$  fall within the  $2\sigma$  uncertainty range for all three lakes (Figure 3b), indicating a simultaneous change in external boundary conditions on the Tibetan Plateau between 11.6 and 11.9 cal. ka BP. The site-specific response at each site is expressed by significant differences in  $\omega_n$  (NC =  $1.44 \pm 0.11$ , TY =  $3.84 \pm 0.89$ , HH =  $0.97 \pm 0.11$ ; supporting information S6), while best fit  $\zeta$  overlap in  $2\sigma$  confidence limits (NC =  $0.20 \pm 0.1$ , TY =  $0.25 \pm 0.1$ , HH =  $0.16 \pm 0.06$ ; supporting information S7).

#### 4. Discussion

The simultaneous step change in the forcing function indicates an abrupt and persistent change in external boundary conditions of the three drainage basins between 11.6 and 11.9 ka BP (Figure 3). The external boundary conditions of landscapes are ultimately determined by the interplay between climate and tectonics (Allen, 2008a). However, displacement rates of alluvial surfaces in the central Kunlun fault system (Van Der Woerd et al., 2002) as well as erosion rates on the southern Tibetan Plateau (Lal et al., 2004) indicate uniform slip and uplift rates for the study areas during the time span of our investigation. Therefore, a tectonic origin of the abrupt change in external boundary conditions is unlikely. Interestingly, the simultaneous change in the forcing function coincides with the termination of the Younger Dryas cold period around  $11.65 \pm 0.1$  ka BP (Walker et al., 2009) (Figure 4). The termination of this cold period has been associated with rapid atmospheric reorganization on the Northern Hemisphere, including rising temperatures in Greenland (Andersen et al., 2004) and major wind shifts over the European continent (Brauer et al., 2008). This reorganization has also been evidenced in both continental and marine climate archives of the Asian continent by an abrupt intensification of monsoonal precipitation (Dykoski et al., 2005; Herzschuh, 2006; Mohtadi et al., 2014; Wang, 2001). Hence, we interpret the step function to reflect an instantaneous shift from glacial to full interglacial climate conditions on the Northern Hemisphere associated with rising Northern Hemisphere temperatures (Figure 4a) and an abrupt intensification of the Asian Monsoon circulation (Figure 4b).

The abrupt increase in temperatures and seasonal precipitation at the termination of the Younger Dryas triggered a transient response in sediment supply in the drainage basins of NC, TY, and HH, characterized by damped oscillations between the deposition of siliciclastic and authigenic sediments. A lake internal origin of these oscillations is unlikely, since neither Holocene changes in water chemistry nor lake level fluctuations exhibit similar variations at lake NC and TY (Ahlborn et al., 2017; Alivernini et al., 2018; Günther et al., 2015). A lake

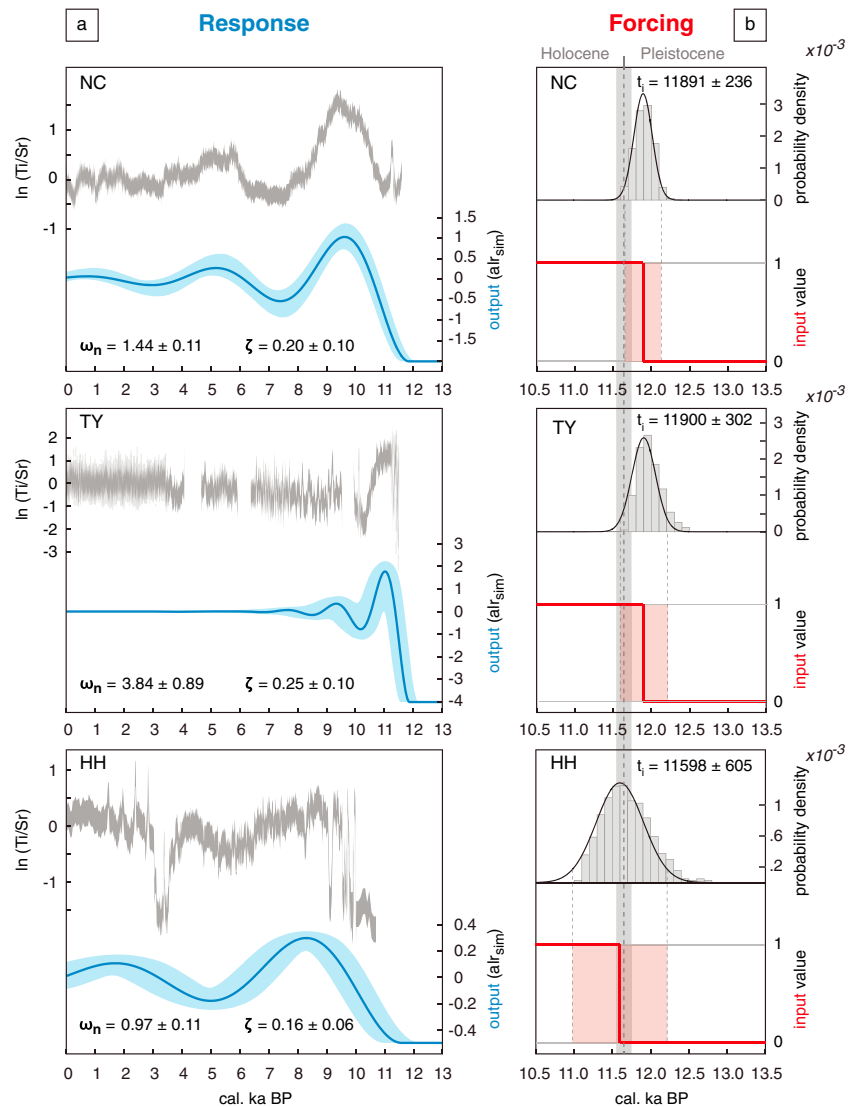


**Figure 3.** Observed and simulated responses in sediment supply to interglacial forcing on the Tibetan Plateau. (a) Relative variations (gray areas) of siliciclastic and authigenic sediment supply ( $\ln(\text{Ti}/\text{Sr})$ ) for Lake Nam Co (NC), Lake Tangra Yumco (TY), and Lake Heihai (HH). Sudden jumps between negative and positive  $\ln(\text{Ti}/\text{Sr})$  values in the record of Lake HH are associated with shifts in the dominant authigenic mineral phase between calcite and aragonite. The median scenarios of the modeled system responses ( $alr_{sim}$ ; blue lines) match the variations indicated by the  $\ln(\text{Ti}/\text{Sr})$  records. Blue envelopes indicate the 95% range of  $10^6$  model scenarios using the estimated parameter uncertainty, whereas the  $\ln(\text{Ti}/\text{Sr})$  records include 95% confidence limits (see supporting information S10). Log-ratio values are normalized by median subtraction. (b) Empirical distribution of initiation times  $t_i$  (gray bars) for best-fit forcing functions (red lines). Red areas denote the  $2\sigma$  uncertainty range of  $t_i$ , as estimated from the empirical distribution.

external origin, in turn, is supported by hydrochemical comparisons between solute concentrations in lake and inflowing waters at NC and TY, which suggest bedrock weathering and transfer by surface and groundwater runoff as primary source of solutes in lake waters (Qiao et al., 2017; Wang et al., 2010). The lakes are strongly depleted in  $\text{Ca}^{2+}$  and  $\text{HCO}_3^{3-}$  resulting in high carbonate precipitation rates (Qiao et al., 2017; J. Wang et al., 2010) and low residence times of alkaline elements in lake waters. Hence, we interpret the oscillations to reflect a feedback between the supply of particulate and solute materials from catchment source areas, which is only possible at the time of sediment release from catchment regolith by erosional processes.

The inferred response model describes particulate and solute supply processes as a feedback loop between two system variables  $x_1$  and  $x_2$  (equation (7)). We interpret the feedback loop to represent an interaction between physical and chemical erosion processes, in which an increase in physical erosion is followed by



## Acknowledgments

This study was financed by the German BMBF project PALMOD—“German Climate Modelling Initiative.” The drilling campaign at Lake Heihai was supported by the DFG project “Tibetan Plateau: Formation—Climate—Ecosystems (TIP).” We thank Torsten Haberzettl and Thomas Kasper for providing the records of Lake Nam Co as well as Marieke Ahlborn for providing the record of Lake Tangra Yumco. The XRF core scanning record of Lake HH (in counts per second) is available at PANGAEA data publisher. We are greatly thankful for the constructive feedback and thorough review by John Armitage and Ken Ferrier.

## References

- Ahlborn, M., Haberzettl, T., Wang, J., Henkel, K., Kasper, T., Daut, G., et al. (2017). Synchronous pattern of moisture availability on the southern Tibetan Plateau since 17.5 cal. ka BP—The Tangra Yumco lake sediment record. *Boreas*, *46*(2), 229–241. <https://doi.org/10.1111/bor.12204>
- Aitchison, J. (1982). The statistical analysis of compositional data. *Journal of the Royal Statistical Society: Series B: Methodological*, *44*(2), 139–177. Retrieved from <http://www.jstor.org/stable/2345821>
- Aitchison, J. (1986). The statistical analysis of compositional data. In *Chapman and Hall* (p. 416). London. <https://doi.org/10.1007/978-94-009-4109-0>
- Akita, L. G., Frenzel, P., Haberzettl, T., Kasper, T., Wang, J., & Reicherter, K. (2015). Ostracoda (Crustacea) as indicators of subaqueous mass movements: An example from the large brackish lake Tangra Yumco on the southern Tibetan Plateau, China. *Palaeogeography, Palaeoclimatology, Palaeoecology*, *419*, 60–74. <https://doi.org/10.1016/j.palaeo.2014.08.003>
- Alivernini, M., Akita, L. G., Ahlborn, M., Börner, N., Haberzettl, T., Kasper, T., et al. (2018). Ostracod-based reconstruction of Late Quaternary lake level changes within the Tangra Yumco lake system (southern Tibetan Plateau). *Journal of Quaternary Science*, *33*(6), 713–720. <https://doi.org/10.1002/jqs.3047>
- Allen, P. A. (2008a). From landscapes into geological history. *Nature*, *451*(7176), 274–276. <https://doi.org/10.1038/nature06586>
- Allen, P. A. (2008b). Time scales of tectonic landscapes and their sediment routing systems. *Geological Society, London, Special Publications*, *296*(1), 7–28. <https://doi.org/10.1144/SP296.2>
- An, F., Lai, Z., Liu, X., Wang, Y., Chang, Q., Lu, B., & Yang, X. (2018). Luminescence chronology and radiocarbon reservoir age determination of lacustrine sediments from the Heihai Lake, NE Qinghai-Tibetan Plateau and its paleoclimate implications. *Journal of Earth Science*, *29*(3), 695–706. <https://doi.org/10.1007/s12583-017-0972-9>
- Andersen, K. K., Azuma, N., Barnola, J. M., Bigler, M., Biscaye, P., Caillon, N., et al. (2004). High-resolution record of Northern Hemisphere climate extending into the last interglacial period. *Nature*, *431*(7005), 147–151. <https://doi.org/10.1038/nature02805>
- Armitage, J. J., Duller, R. A., Whittaker, A. C., & Allen, P. A. (2011). Transformation of tectonic and climatic signals from source to sedimentary archive. *Nature Geoscience*, *4*(4), 231–235. <https://doi.org/10.1038/ngeo1087>
- Armitage, J. J., Dunkley Jones, T., Duller, R. A., Whittaker, A. C., & Allen, P. A. (2013). Temporal buffering of climate-driven sediment flux cycles by transient catchment response. *Earth and Planetary Science Letters*, *369–370*, 200–210. <https://doi.org/10.1016/j.epsl.2013.03.020>
- Bonnet, S., & Crave, A. (2003). Landscape response to climate change: Insights from experimental modeling and implications for tectonic versus climatic uplift of topography. *Geology*, *31*(2), 123–126. [https://doi.org/10.1130/0091-7613\(2003\)031<0123:LRCCI>2.0.CO](https://doi.org/10.1130/0091-7613(2003)031<0123:LRCCI>2.0.CO)
- Bradley, E., & Kantz, H. (2015). Nonlinear time-series analysis revisited. *Chaos*, *25*(9), 097610. <https://doi.org/10.1063/1.4917289>
- Brauer, A., Haug, G. H., Dulski, P., Sigman, D. M., & Negendank, J. F. W. (2008). An abrupt wind shift in western Europe at the onset of the Younger Dryas cold period. *Nature Geoscience*, *1*(August), 520–523. <https://doi.org/10.1038/ngeo263>
- Dalman, R., Weltje, G. J., & Karamitopoulos, P. (2015). High-resolution sequence stratigraphy of fluvio-deltaic systems: Prospects of system-wide chronostratigraphic correlation. *Earth and Planetary Science Letters*, *412*, 10–17. <https://doi.org/10.1016/j.epsl.2014.12.030>
- Doberschütz, S., Frenzel, P., Haberzettl, T., Kasper, T., Wang, J., Zhu, L., et al. (2014). Monsoonal forcing of Holocene paleoenvironmental change on the central Tibetan Plateau inferred using a sediment record from Lake Nam Co (Xizang, China). *Journal of Paleolimnology*, *51*(2), 253–266. <https://doi.org/10.1007/s10933-013-9702-1>
- Dykoski, C. A., Edwards, R. L., Cheng, H., Yuan, D., Cai, Y., Zhang, M., et al. (2005). A high-resolution, absolute-dated Holocene and deglacial Asian monsoon record from Dongge cave, China. *Earth and Planetary Science Letters*, *233*(1–2), 71–86. <https://doi.org/10.1016/j.epsl.2005.01.036>
- Engstrom, D. R., Fritz, S. C., Almendinger, J. E., & Juggins, S. (2000). Chemical and biological trends during lake evolution in recently deglaciated terrain. *Nature*, *408*(6809), 161–166. <https://doi.org/10.1038/35041500>
- Ferrier, K. L., & Kirchner, J. W. (2008). Effects of physical erosion on chemical denudation rates: A numerical modeling study of soil-mantled hillslopes. *Earth and Planetary Science Letters*, *272*(3–4), 591–599. <https://doi.org/10.1016/j.epsl.2008.05.024>
- Ferrier, K. L., & West, N. (2017). Responses of chemical erosion rates to transient perturbations in physical erosion rates, and implications for relationships between chemical and physical erosion rates in regolith-mantled hillslopes. *Earth and Planetary Science Letters*, *474*, 447–456. <https://doi.org/10.1016/j.epsl.2017.07.002>
- Gabet, E. J., & Mudd, S. M. (2009). A theoretical model coupling chemical weathering rates with denudation rates. *Geology*, *37*(2), 151–154. <https://doi.org/10.1130/G25270A.1>
- Günther, F., Witt, R., Schouten, S., Mäusbacher, R., Daut, G., Zhu, L., et al. (2015). Quaternary ecological responses and impacts of the Indian Ocean summer monsoon at Nam Co, southern Tibetan Plateau. *Quaternary Science Reviews*, *112*, 66–77. <https://doi.org/10.1016/j.quascirev.2015.01.023>
- Haberzettl, T., Henkel, K., Kasper, T., Ahlborn, M., Su, Y., Wang, J., et al. (2015). Independently dated paleomagnetic secular variation records from the Tibetan Plateau. *Earth and Planetary Science Letters*, *416*, 98–108. <https://doi.org/10.1016/j.epsl.2015.02.007>
- Heimsath, A. M. (2012). Quantifying processes governing soil-mantled hillslope evolution. In *Hydrogeology* (pp. 205–242). Amsterdam, Netherlands: Elsevier. <https://doi.org/10.1016/B978-0-12-386941-8.00007-1>
- Henkel, K., Haberzettl, T., St-Onge, G., Wang, J., Ahlborn, M., Daut, G., et al. (2016). High-resolution paleomagnetic and sedimentological investigations on the Tibetan Plateau for the past 16 ka cal B.P.—The Tangra Yumco record. *Geochemistry, Geophysics, Geosystems*, *17*, 774–790. <https://doi.org/10.1002/2015GC006023>
- Herzschuh, U. (2006). Palaeo-moisture evolution in monsoonal Central Asia during the last 50,000 years. *Quaternary Science Reviews*, *25*(1–2), 163–178. <https://doi.org/10.1016/j.quascirev.2005.02.006>
- Humphrey, N. F., & Heller, P. L. (1995). Natural oscillations in coupled geomorphic systems: An alternative origin for cyclic sedimentation. *Geology*, *23*(6), 499–502. [https://doi.org/10.1130/0091-7613\(1995\)023<0499:NOICGS>2.3.CO](https://doi.org/10.1130/0091-7613(1995)023<0499:NOICGS>2.3.CO)
- Jarvis, A., Reuter, H. I., Nelson, A., & Guevara, E. (2008). Hole-filled SRTM for the globe version 4. Available from the CGIAR-CSI SRTM 90m Database (<http://Srtm.Csi.Cgiar.Org>).
- Jerolmack, D. J., & Paola, C. (2010). Shredding of environmental signals by sediment transport. *Geophysical Research Letters*, *37*, L19401. <https://doi.org/10.1029/2010GL044638>
- Kasper, T., Haberzettl, T., Doberschütz, S., Daut, G., Wang, J., Zhu, L., et al. (2012). Indian Ocean summer monsoon (IOSM)-dynamics within the past 4 ka recorded in the sediments of Lake Nam Co, central Tibetan Plateau (China). *Quaternary Science Reviews*, *39*(August), 73–85. <https://doi.org/10.1016/j.quascirev.2012.02.011>
- Kennel, M. B., Brown, R., & Abarbanel, H. D. I. (1992). Determining embedding dimension for phase-space reconstruction using a geometrical construction. *Physical Review A*, *45*(6), 3403–3411. <https://doi.org/10.1103/PhysRevA.45.3403>

- Kim, W., & Jerolmack, D. J. (2008). The pulse of calm fan deltas. *The Journal of Geology*, 116(4), 315–330. <https://doi.org/10.1086/588830>
- Lal, D., Harris, N. B. W., Sharma, K. K., Gu, Z., Ding, L., Liu, T., et al. (2004). Erosion history of the Tibetan Plateau since the last interglacial: Constraints from the first studies of cosmogenic  $^{10}\text{Be}$  from Tibetan bedrock. *Earth and Planetary Science Letters*, 217(1–2), 33–42. [https://doi.org/10.1016/S0012-821X\(03\)00600-9](https://doi.org/10.1016/S0012-821X(03)00600-9)
- Lockett, G., Ramisch, A., Wünnemann, B., Hartmann, K., Haberzettl, T., Chen, H., & Diekmann, B. (2015). A process- and provenance-based attempt to unravel inconsistent radiocarbon chronologies in lake sediments: An example from Lake Heihai, north Tibetan Plateau (China). *Radiocarbon*, 57(05), 1003–1019. [https://doi.org/10.2458/azu\\_rc.57.18221](https://doi.org/10.2458/azu_rc.57.18221)
- Long, H., Haberzettl, T., Tsukamoto, S., Shen, J., Kasper, T., Daut, G., et al. (2015). Luminescence dating of lacustrine sediments from Tangra Yumco (southern Tibetan Plateau) using post-IR IRSL signals from polymineral grains. *Boreas*, 44(1), 139–152. <https://doi.org/10.1111/bor.12096>
- Lu, X., Herrmann, M., Mosbrugger, V., Yao, T., & Zhu, L. (2010). Airborne pollen in the Nam Co Basin and its implication for palaeoenvironmental reconstruction. *Review of Palaeobotany and Palynology*, 163(1–2), 104–112. <https://doi.org/10.1016/j.revpalbo.2010.10.004>
- Marwan, N., Carmen Romano, M., Thiel, M., & Kurths, J. (2007). Recurrence plots for the analysis of complex systems. *Physics Reports*, 438(5–6), 237–329. <https://doi.org/10.1016/j.physrep.2006.11.001>
- Miehe, S., Miehe, G., van Leeuwen, J. F. N., Wroczynna, C., van der Knaap, W. O., Duo, L., & Haberzettl, T. (2014). Persistence of Artemisia steppe in the Tangra Yumco Basin, west-central Tibet, China: Despite or in consequence of Holocene lake-level changes? *Journal of Paleolimnology*, 51(2), 267–285. <https://doi.org/10.1007/s10933-013-9720-z>
- Mischke, S., Weynell, M., Zhang, C., & Wiechert, U. (2013). Spatial variability of  $^{14}\text{C}$  reservoir effects in Tibetan Plateau lakes. *Quaternary International*, 313, 147–155.
- Mohtadi, M., Prange, M., Oppo, D. W., De Pol-Holz, R., Merkel, U., Zhang, X., et al. (2014). North Atlantic forcing of tropical Indian Ocean climate. *Nature*, 509(7498), 76–80. <https://doi.org/10.1038/nature13196>
- Müller, C., & Kürschner, H. (2014). Phytosociological and palynological studies of alpine steppe communities on the northern Tibetan Plateau, Qinghai Province, China. *Feddes Repertorium*, 124(4), 122–138. <https://doi.org/10.1002/fedr.201400006>
- Ott, F., Kramkowski, M., Wulf, S., Plessen, B., Serb, J., Tjallingii, R., et al. (2017). Site-specific sediment responses to climate change during the last 140 years in three varved lakes in northern Poland. *The Holocene*, 28(3), 464–477. <https://doi.org/10.1177/0959683617729448>
- Packard, N. H., Crutchfield, J. P., Farmer, J. D., & Shaw, R. S. (1980). Geometry from a time series. *Physical Review Letters*, 45(9), 712–716. <https://doi.org/10.1103/PhysRevLett.45.712>
- Phillips, C. L., Parr, J. M., & Riskin, E. A. (1995). *Signals, systems, and transforms*. Upper Saddle River, NJ: Prentice Hall.
- Phillips, J. D. (2007). The perfect landscape. *Geomorphology*, 84(3–4), 159–169. <https://doi.org/10.1016/j.geomorph.2006.01.039>
- Qiao, B., Wang, J., Huang, L., & Zhu, L. (2017). Characteristics and seasonal variations in the hydrochemistry of the Tangra Yumco basin, central Tibetan Plateau, and responses to the Indian summer monsoon. *Environmental Earth Sciences*, 76(4), 1–13. <https://doi.org/10.1007/s12665-017-6479-y>
- Ramisch, A., Lockett, G., Haberzettl, T., Hartmann, K., Kuhn, G., Lehmkühl, F., et al. (2016). A persistent northern boundary of Indian summer monsoon precipitation over central Asia during the Holocene. *Scientific Reports*, 6(1), 25791. <https://doi.org/10.1038/srep25791>
- Roberts, N., Allcock, S. L., Arnaud, F., Dean, J. R., Eastwood, W. J., Jones, M. D., et al. (2016). A tale of two lakes: A multi-proxy comparison of late glacial and Holocene environmental change in Cappadocia, Turkey. *Journal of Quaternary Science*, 31(4), 348–362. <https://doi.org/10.1002/jqs.2852>
- Romans, B. W., Castellort, S., Covault, J. A., Fildani, A., & Walsh, J. P. (2016). Environmental signal propagation in sedimentary systems across timescales. *Earth-Science Reviews*, 153, 7–29. <https://doi.org/10.1016/j.earscirev.2015.07.012>
- Stauch, G., Schulte, P., Ramisch, A., Hartmann, K., Hülle, D., Lockett, G., et al. (2017). Landscape and climate on the northern Tibetan Plateau during the late Quaternary. *Geomorphology*, 286, 78–92. <https://doi.org/10.1016/j.geomorph.2017.03.008>
- Strogatz, S. H. (2001). *Nonlinear dynamics and chaos: With applications to physics, biology, chemistry, and engineering*. Boulder, CO: Westview Press. <https://doi.org/10.1201/9780429492563>
- Takens, F. (1981). Detecting strange attractors in turbulence. In *Dynamical systems and turbulence, Warwick 1980* (pp. 366–381). Berlin Heidelberg New York: Springer.
- Tjallingii, R., Röhl, U., Kölling, M., & Bickert, T. (2007). Influence of the water content on X-ray fluorescence corescanning measurements in soft marine sediments. *Geochemistry, Geophysics, Geosystems*, 8, 1–12. <https://doi.org/10.1029/2006GC001393>
- Van Der Woerd, J., Tapponnier, P., Ryerson, F. J., Meriaux, A. S., Meyer, B., Gaudemer, Y., et al. (2002). Uniform postglacial slip-rate along the central 600 km of the Kunlun fault (Tibet), from  $^{26}\text{Al}$ ,  $^{10}\text{Be}$ , and  $^{14}\text{C}$  dating of riser offsets, and climatic origin of the regional morphology. *Geophysical Journal International*, 148(3), 356–388. <https://doi.org/10.1046/j.1365-246x.2002.01556.x>
- Walker, M., Johnsen, S., Rasmussen, S. O., Popp, T., Steffensen, J. P., Gibbard, P., et al. (2009). Formal definition and dating of the GSSP (Global Stratotype Section and Point) for the base of the Holocene using the Greenland NGRIP ice core, and selected auxiliary records. *Journal of Quaternary Science*, 24(1), 3–17. <https://doi.org/10.1002/jqs.1227>
- Wang, J., Zhu, L., Wang, Y., Ju, J., Xie, M., & Daut, G. (2010). Comparisons between the chemical compositions of lake water, inflowing river water, and lake sediment in Nam Co, central Tibetan Plateau, China and their controlling mechanisms. *Journal of Great Lakes Research*, 36(4), 587–595. <https://doi.org/10.1016/j.jglr.2010.06.013>
- Wang, Y. J. (2001). A high-resolution absolute-dated Late Pleistocene monsoon record from Hulu cave, China. *Science*, 294(5550), 2345–2348. <https://doi.org/10.1126/science.1064618>
- Weltje, G. J., & Tjallingii, R. (2008). Calibration of XRF core scanners for quantitative geochemical logging of sediment cores: Theory and application. *Earth and Planetary Science Letters*, 274(3–4), 423–438. <https://doi.org/10.1016/j.epsl.2008.07.054>
- Weltje, G. J., Bloemsa, M. R., Tjallingii, R., Heslop, D., Röhl, U., & Croudace, I. W. (2015). Micro-XRF Studies of Sediment Cores. In *Micro-XRF Studies of Sediment Cores* (Vol. 17, pp. 25–35). <https://doi.org/10.1007/978-94-017-9849-5>
- Wischniewski, J., Mischke, S., Wang, Y., & Herzschuh, U. (2011). Reconstructing climate variability on the northeastern Tibetan Plateau since the last late glacial—A multi-proxy, dual-site approach comparing terrestrial and aquatic signals. *Quaternary Science Reviews*, 30(1–2), 82–97. <https://doi.org/10.1016/j.quascirev.2010.10.001>